The influence of a plate obstacle on the burning behavior of small scale pool fires: an experimental study

Jian Chen[1], Ye Song[1], Yueyang Yu[1], Guoqing Xiao[2,3], Wai Cheong Tam[4], Depeng Kong [1,]*

[1]Center for Offshore Engineering and Safety Technology, China University of Petroleum (East China), Qingdao 266580, China

[2]College of Chemistry and Chemical Engineering, Southwest Petroleum University, Chengdu 610500, China

[3] State Key Laboratory of Oil and Gas Reservoir Geology and Exploitation, Southwest Petroleum University, Chengdu 610500, China

[4]Fire Research Division, National Institute of Standards and Technology, Gaithersburg, MD 20899, United States

Corresponding author: Prof. Depeng Kong; E-mail: kongdepeng@upc.edu.cn

Abstract

For a typical thermal runaway process of uncontrolled energy release, pool fires are typically associated with the safety of energy application in modern production and life. In order to improve fire safety in energy utilization, it is significant to investigate the burning behavior of pool fire incorporating burning rate and flame characteristic, which are fundamental parameters in hazard prediction and risk management. Although there are different obstructions in real industrial fire scenarios, nearly no work has been conducted to explore the influence of obstruction on pool fires. Aiming at characterizing the influence of a plate obstacle on pool fire, a series of small-scale pool fires affected by plate obstacle are performed. The findings show the plate obstacle above the burner has a considerable effect on the burning behaviors of n-heptane and ethanol pool fires. The plate obstacle over the burner would result in a rapidly developing fire with higher burning rate. The external radiation from plate obstacle to the fuel surface was found to be responsible for the burning rate enhancement through the heat transfer analysis. Furthermore, based on the theoretical

and scaling analysis, a new correlation for burning rate is proposed to describe the effect of plate obstacle, and the relationship between mean radiation heat flux and the characteristics of plate obstacle is revealed. It is expected this work will help to understand the burning behavior of pool fires in a more realistic fire setting.

Keywords

Pool fire; Plate obstacle; Burning behavior; Burning rate

Nomenclature

B	diffusive transfer number	N	Nusselt number
B_f	ratio of the diameter of obstacle to the height of obstacle	Pr	Prandtl number
		$\dot{q}''_{cond}$	conductive heat transfer
B_o	ratio of the diameter of fuel pool to the height of obstacle	$\dot{q}''_{l}$	heat loss
		$\dot{q}''_{mean}$	mean radiation heat flux
c_p	heat capacity	$\dot{q}''_{r,f}$	radiative heat transfer
$c_{p,l}$	Specific heat	$\dot{q}''_{r,o}$	external heat feedback from plate
d	diameter of obstacle	T_b	Boiling temperature
D	diameter of the fuel pool	T_f	flame temperature near the fuel pan
$F_{o\text{-}f}$	view factor	T_o	temperature of the plate obstacle
Gr	Grashof number	T_∞	environmental temperature
h	plate obstacle height	t_{boilin}	time from ignition to boiling
h_f	convective heat transfer	t_{peak}	time from ignition to peak burning rate
h_{fg}	latent heat of vaporization	t_{total}	time from ignition to extinguish
H_c	heat of combustion	α_f	flame absorption
H_g	latent heat of gasification	ΔH_c	Heat of combustion
H_v	gasification heat	$\Delta\dot{m}''$	increased burning rate
k	coefficient of thermal	σ	Stefan–Boltzmann constant
L	heat of gasification	ε_o	obstacle emissivity
$\dot{m}''$	burning rate		

1. Introduction

Since the industrial revolution, oil has been powering the social development and economic growth for over 150 years. It is reported the oil currently supplies about 30 percent of the overall energy consumption around the world, and will remain an indispensable part in the future [1, 2]. Along with the development of petroleum-chemical industry involved with a large number of flammable and explosive materials, the environmental and safety issues (such as global warming, fire and explosion) have become the primary challenges and have attracted increasing attention from many researchers [3-6]. As one of the most serious disasters of flammable liquid leakage, pool fires are typically associated with the safety of liquid fuel in modern production and life [7, 8]. This typical fire ordinarily happens as the flammable liquid pool is formed followed by the storage tanks or transport pipelines leakage, and then gets ignited. In such an accident, the heat transfers to surrounding equipment by convection and radiation and the combustion product releases to the nearby space, which directly pose a great threat to people's safety and also the environment. Moreover, the heat release of pool fire can subsequently ignite the surrounding combustible materials and cause the secondary accidents, such as those appeared in the BP Deepwater Horizon explosion and the Jaipur fire accident [9-]12]. It was reported by Reniers et al. [9] that pool fire accounts for 44 percent of all accidents triggering a domino event (i.e. higher-order accident). Therefore, quantifying burning parameters of pool fires plays an important role for the fire safety in energy utilization.

The thermal hazard of pool fire changes with complicated fire scenarios. Hence, the understanding burning parameters of pool fires in various scenarios is fundamental research area for the hazard prediction and risk analysis [13-16]. A number of research efforts on the burning behavior of pool fires with various boundary conditions have been

carried out in recent years, including pool scale [17], initial fuel temperature [18, 19], lip height (the distance from fuel surface to the burner rim) [20] and geometry of fuel pool [2, 21-23]. As one of the most important burning parameters, the burning rate depends on the heat feedback from pool fire. In the classic scaling model built by Blinov and Khudyakov [17], three regimes are defined based on the dominant heat feedback. For conduction-dominant pool fire with circular pool diameter, D, smaller than 7 cm, the burning rate decreases with scale. With the increase of scale, the dominant heat transfer change from the convection (7 cm < D < 20 cm) to the radiation (D > 20 cm), thus resulting that the burning rate increases and approaches a constant finally. Lu et al. [18] explored the effect of initial fuel temperature, where unsteady evolution process of pool fire was observed and four burning stages were defined. Their results showed that the increase of initial fuel temperature would accelerate boiling and results in a significant increase of burning intensity. Considering the floating sealing annular pool generally formed in tank fire scenario, Tang et al. [22] presented experimental data and physical model for the prediction of flame height. More recently, Deng et al. [2, 21] investigated the burning rate of annular pool fire with various diameter. An increasing trend in burning rate was found, and was explained by dimensional analysis with fuel mass transfer number.

Burning behavior of pool fires can also be affected by the ambient conditions, such as ambient pressure [24-27], cross flow [28-30], oxygen concentration and humidity [31, 32]. Due to the requirement for fire safety in high altitude conditions, the effect of pressure on pool fire burning has been investigated widely[24-27]. The exponential relationship between burning rate and environmental pressure has been verified through experimental data from field tests and bench-scale pressure chambers, where the exponent value in the

exponential relationship changes with the scale of pool fire [26]. Considering fire condition usually involving winds, Hu et al. [28-30] performed detailed investigations on the impact of cross flow on pool fire with various pool diameter. They revealed that the cross flow would influence the heat feedback mechanisms and the fuel-air mixing, resulting non-monotonic change in burning rate. Recently, Zhang et al. [32] presented experimental results on the pool fire for bench-scale experiments using a closed chamber with a wide range of initial temperature and relative humidity conditions. Their results showed that the burning rate would decrease with decreasing initial temperature or increasing relative humidity. Chen et al. [31] experimentally found the oxygen concentrations affect the evolution process of pool fire significantly. As the oxygen concentrations increase, the boiling burning phase appear earlier with higher heat release rate.

The previous works provide important insights for burning behavior of free burning pool fires in various scenarios. However, as there are lots of obstructions in real industrial fire scenarios, the understanding of pool fire burning affected by obstruction became a significant research. In principle, near-by obstacles to the fuel pool will affect the fire development of pool fire and subsequently change the thermal hazard of pool fire to the surrounding environment. Recently, some studies [33, 34] have been conducted for jet fire under the influence of obstacle. Ji et al. [33] established a flame size model to predict behaviors of the horizontal jet flame after it impinges the wall, which could collapse the longitudinal length of the flame impinging the wall. Zhou et al. [34] derived an equation of fire plume upward flowing along the plate, with the flame plume radius as the characteristic length scale, which could accurately predict temperature data in whole impinging zone. However, nearly no work has been done to explore the influence of

obstruction on pool fires. As mentioned above, the burning rate of pool fire without the effect of obstacle, i.e. free burning pool fire, is determined based on the heat feedback from pool fire. For pool fire sheltered by an obstacle such as a circular flat plate, the burning rate is likely to be driven by the combination of heat feedback from the flame and the obstacle. Moreover, the obstacle is expected to change the flame appearance and radiation and to introduce a splitting flame phenomenon in which influence the evolution process of pool fire significantly.

Aiming at filling these knowledge gaps, the influence of obstacle on the burning characteristic of pool fires was investigated, where the complex obstacle configuration in the real fire scenarios was simplified to the circular plate obstacle above the burner. The 10 cm diameter heptane and ethanol pool fires affected by a plate obstacle were performed, and the burning characteristics were analyzed. The main novel contribution of this work is that a new correlation for burning rate is proposed to describe the effect of plate obstacle. In addition, the relationship between mean radiation heat flux of pool fire and the characteristics of plate obstacle is revealed. The established model improves the understanding for burning parameters of real industrial pool fire scenarios involved with obstacles. Further, this work could provide a data support and theoretical basis to estimate the heat release rate and calculate the safety distance between fire area and surrounding environment, which might provide new reference for reducing the damage caused by fire and improving the safety of energy application.

2 Theoretical analysis

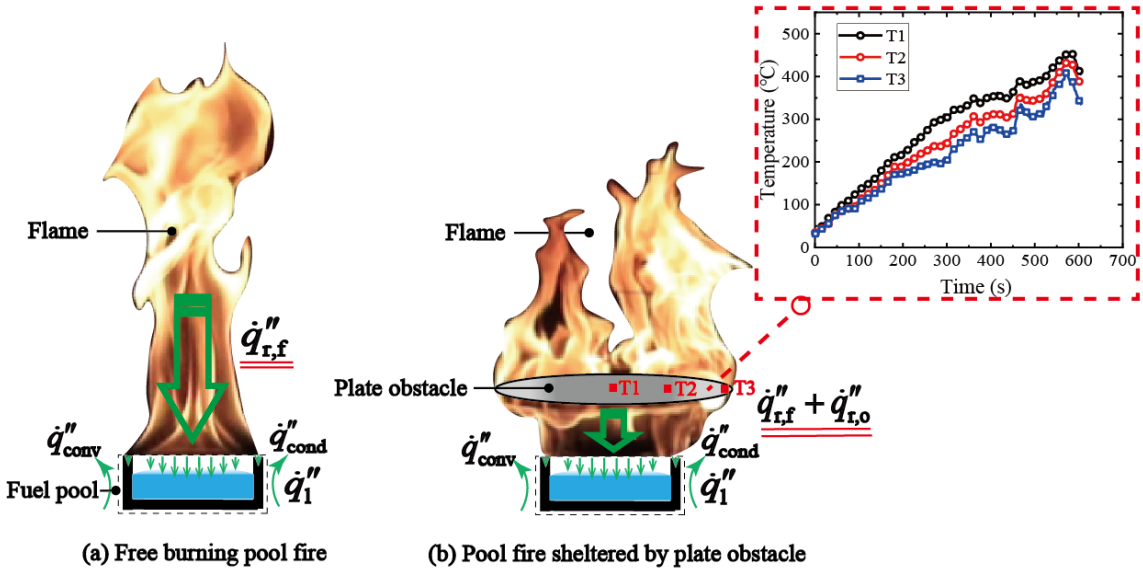

Fig. 1 The schematic diagrams of heat transfer for (a) pool fire under the free burning condition (b) pool fire under the effect of plate obstacle

The burning rate is determined by the total heat feedback received by the surface of fuel pool during the combustion process. The more heat feedback would lead to the more fuel vapor evaporated from the surface of the liquid fuel, corresponding to the greater burning rate. The schematic diagrams of heat transfer for pool fire under the free burning condition and pool fire under the effect of plate obstacle are shown in Fig. 1.

For pool fire under the free burning condition, the burning rate can be expressed as

$$\dot{m}'' \propto \dot{q}''_{\mathrm{cond}} + \dot{q}''_{\mathrm{conv}} + \dot{q}''_{\mathrm{r,f}} - \dot{q}''_{\mathrm{l}} \tag{1}$$

where $\dot{q}''_{\mathrm{cond}}$ is conductive heat transfer item, $\dot{q}''_{\mathrm{conv}}$ is convective heat transfer item, $\dot{q}''_{\mathrm{r,f}}$ is radiative heat transfer item, and $\dot{q}''_{l}$ is heat loss item. For 10 cm diameter pool fire, the dominant heat transfer items are $\dot{q}''_{\mathrm{cond}}$ and $\dot{q}''_{\mathrm{conv}}$.

$\dot{q}''_{\mathrm{cond}}$ is written as

$$\dot{q}''_{\text{cond}} \propto k(T_f - T_b) \tag{2}$$

where T_f and T_b are flame temperature near the burner and boiling temperature, respectively.

$\dot{q}''_{\text{conv}}$ is expressed as

$$\dot{q}''_{\text{conv}} \propto h_{\text{f}}(T_f - T_b) \tag{3}$$

where h_{f} i.e. convective heat transfer coefficient could be calculated as $h \propto Nu^n \propto (\text{Pr} \cdot Gr)^n$. The Pr number depends on the fluid properties. The Gr number represents the ratio of the buoyancy to viscous force, and would increase when the flow around fuel burner changes to turbulent [35].

For the pool fire under the effect of plate obstacle, the temperature of plate obstacle increases significantly from ambient temperature. The received heat flux of fuel pool not only includes the heat feedback of the flame, but also the radiation heat feedback of the plate obstacle. Considering the external heat transfer from the plate obstacle, i.e. $\dot{q}''_{\text{r,o}}$, the burning rate is expressed as

$$\dot{m}'' \propto \dot{q}''_{\text{cond}} + \dot{q}''_{\text{conv}} + \dot{q}''_{\text{r,f}} + \dot{q}''_{\text{r,o}} - \dot{q}''_{\text{l}} \tag{4}$$

The external heat feedback from plate obstacle, i.e. $\dot{q}''_{\text{r,o}}$ could be calculated as

$$\dot{q}''_{\text{r,o}} = F_{\text{o-f}} \sigma \varepsilon_o (1 - \alpha_f) T_{\text{o}}^4 \tag{5}$$

where the term $F_{\text{o-f}}$ represents the view factor between the plate obstacle and fuel pool, σ is Stefan–Boltzmann constant, ε_o is the obstacle emissivity, α_f is the flame absorption, T_{o} is the temperature of the plate obstacle.

$F_{\text{o-f}}$ would change with the height of plate obstacle and the diameter of the plate obstacle, and could be calculated as

$$F_{\text{o-f}} = \frac{1}{2}\left\{ X - \left[X^2 - 4\left(\frac{B_{\text{f}}}{B_{\text{o}}}\right)^2 \right]^{1/2} \right\} \tag{6}$$

where B_{f} represents the ratio of the diameter of obstacle to the height of obstacle, i.e. d/h, B_{o} represents the ratio of the diameter of fuel pool to the height of obstacle, i.e. D/h, and X is calculated as $X = 1 + \frac{1 + B_{\text{f}}^2}{B_{\text{o}}^2}$.

The external radiation of plate obstacle would increase the burning rate. In the heat transfer of pool fire, it is assumed that the obstacle has limited effect on the heat transfer from pool fire to liquid fuel. So, the increased burning rate for pool fire under the effect of plate obstacle is mainly caused by the external radiation from plate obstacle. The increased burning rate is calculated by $\Delta\dot{m}'' = \dot{m}'' - \dot{m}_0''$, where $\dot{m}_0''$ is the burning rate of pool fire under the free burning condition. The theoretical value of increased burning rate caused by the obstacle could be calculated as

$$\Delta\dot{m}'' = \frac{\dot{q}_{\text{r,o}}''}{H_v + c_p(\text{T}_b - \text{T}_\infty)} = \frac{F_{\text{o-f}}\sigma\varepsilon_f(1-\alpha_f)T_{\text{o}}^4}{H_v + c_p(\text{T}_b - \text{T}_\infty)} \tag{7}$$

3 Experimental apparatus and procedures

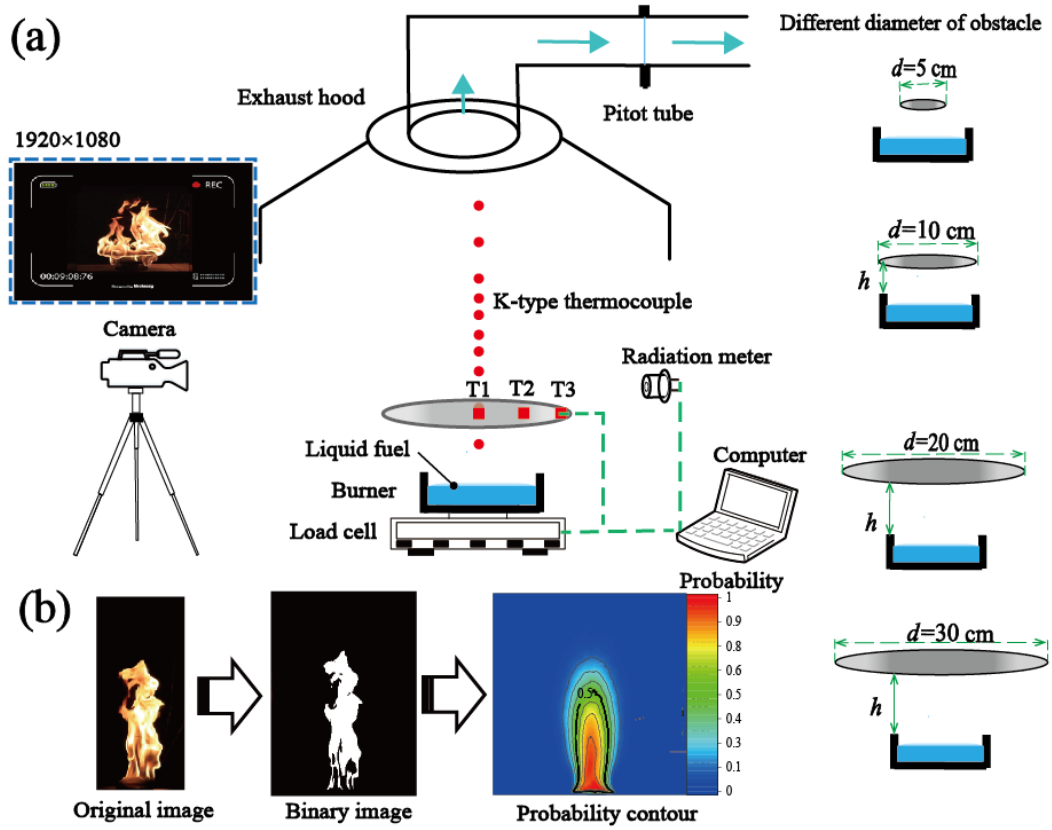

Fig. 2 Experimental setup

In the current study, pool fire was burned under a quiescent environment. The burner was positioned under the center of smoke exhaust hood (3 m x 3 m), where the flow rate of smoke exhaust was kept at constant and it was approximately 0.4 kg/s. The schematic of the experimental platform of small-scale pool fire is shown in the Fig. 2 and it is composed of the fuel pool sheltered by plate obstacle and burning parameter measurement system.

Small-scale pool fires were conducted in a 10 cm diameter steel pan with a depth of 3.5 cm. The pan thickness is 0.2 cm ± 0.01 cm. N-heptane (C_7H_{16}) and ethanol (C_2H_6O) were chosen as the burning fuel. The properties of liquid fuels are listed in Table 1. The initial lip height was controlled as 1.5 cm for all experimental conditions. Noted that the

lip height would increase with the consumption of liquid fuel, so the unsteady state burning process from ignition to the burn-out can be observed. A circular stainless steel plate is used as the obstacle. The thickness of the circular plate is about 4 mm and it is located above the pool surface. Four different sizes of circular plates are also considered and they are 5, 10, 20 and 30 cm. The circle stainless steel plate was suspended above the fuel pool.

Table 1 The properties of liquid fuels

Name	Symbol	Materials and value		Unit
		Ethanol	n-Heptane	
Specific heat	$c_{p,l}$	3030[36]	2470[37]	J/(kg.K)
Boiling temperature	T_b	351.5[38]	371.4[38]	K
Heat of combustion	ΔH_c	26.8[38]	44.6[38]	kJ/g
Heat of gasification	L	891[38]	448[38]	kJ/kg
Latent heat of vaporization	h_{fg}	837[38]	316[38]	kJ/kg

The measurement system was used to characterize the burning behavior. The mass loss rate was obtained by an electronic balance and it was positioned directly under the burner. For the configurations of the electronic balance, the maximum measurement value and its resolution were 6200 g and 0.01 g, respectively. The plate temperature at different locations was monitored by three K-type patch thermocouples (labeled as T1, T2, T3 in Figs. 2). T1 was placed at the center of the plate. T3 was positioned near the edge of the plate and T2 was located in between T1 and T3. Besides, there were 10 K-type thermocouples measuring the flame temperature at different vertical locations. The resolution of the thermocouples with 1 mm diameter was about 1 K. A wide-angle radiometer was used to

measure the local heat flux, and the distance between radiometer central axis of burner keeps 60 cm.

A digital camera was utilized to record the entire development process of pool fire. The camera was placed about 70 cm vertically away from the floor and 260 cm horizontally away from the center of the fuel pool. The camera settings were manually adjusted to obtain high-quality pool fire videos. These settings included the ISO number and F number. Using the recorded videos, the frame-by-frame geometry of the pool fire flame, as shown in Fig. 2(b) was extracted using an in-house code written in MATLAB. Followed by the image processing method [39], flame area in these pictures were identified. For the same frame photo, the original picture and binary picture were compared in Fig. 3 (b). Lastly, the flame probability contour was calculated and plotted as shown in Fig. 3 (b).

There were two varying parameters: the relative height, h, the distance between the pool surface and the circular plate and the plate diameter, d. Six different relative heights were considered (i.e., h = 5, 10, 20, 30, 40 and 60 cm) and four different plate diameters (i.e., d = 5, 10, 20 and 30 cm) were accounted for. Each of the experiments was repeated for at least two times for repeatability. During the test, the ambient temperature was observed to be about 298 K - 303 K. Each experiment test was conducted for 2-3 times, and the experimental data presented in section 3 was the mean value of repeatable tests.

The total uncertainty of measuring burning rate was principally caused by two factors, including the repeatability error of experiments and reading precision error of electronic balance. Based on the burning rate values obtained in the repeated experiments, the repeatability error was found to be about 8%. The reading precision error of electronic balance was within 5%. The overall uncertainty of burning rate was obtained as 9.4%

according to the Moffat's method [40], which was generally used in the uncertainty calculation for fire burning parameters [41, 42].

3 Results and discussion

3.1 Burning behavior of the pool fire

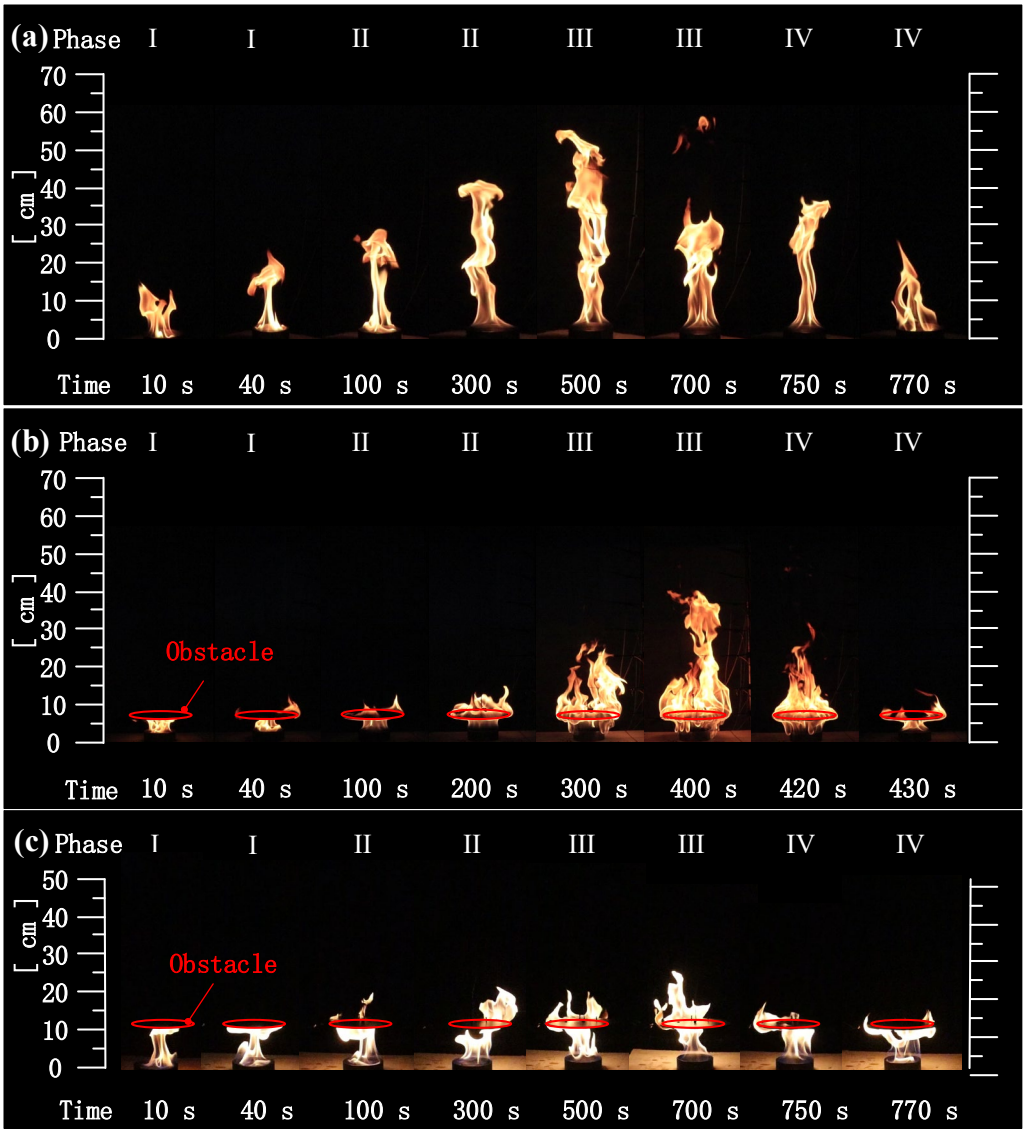

Fig. 3 Flame appearance evolution for (a) free burning n-heptane pool fire and (b) n-heptane pool fire with plate obstacle (d=20 cm, h=10 cm) (c) ethanol pool fire with plate obstacle (d=20 cm, h=10 cm)

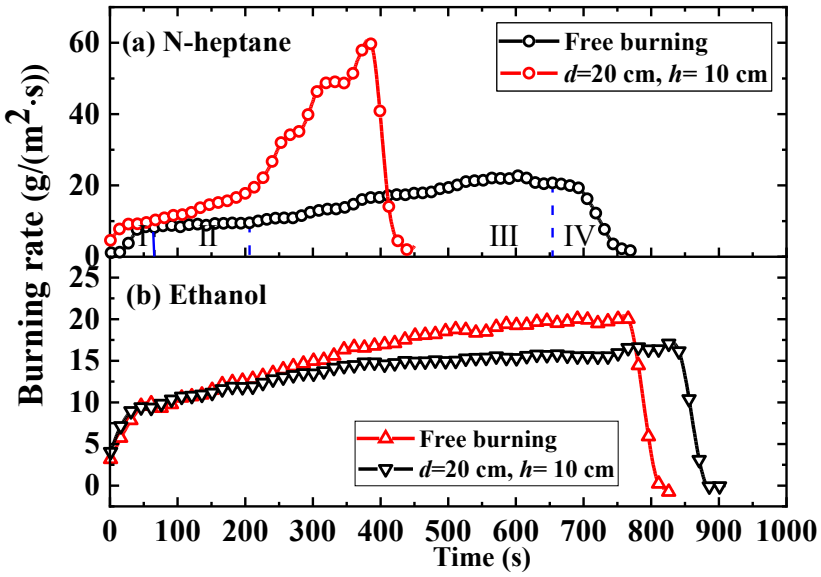

Fig. 4 The development of burning rate for pool fire under the free burning condition and pool fire under the effect of plate obstacle (d=20 cm, h=10 cm)

A typical view of the flame appearance for pool fire with plate obstacle (d = 20 cm, h = 10 cm) is presented in the Fig. 3, where the pool fire under the free burning condition is also presented as the comparison. Fig. 4 presents the measured burning rate evolution with time for these conditions. The plate obstacle above the burner has a considerable effect on the burning behaviors of n-heptane and ethanol pool fires. The change of burning characteristic with time is more distinct for pool fire burning n-heptane, which is consistent with previous results [13]. Furthermore, the unsteady burning evolution of n-heptane pool fire is discussed in this section. According to the evolution of burning rate and flame appearance, the development of n-heptane pool fire is divided into the following four phases:

(1) The phase of ignition. The duration of this phase is very short, where the burning rate and flame area increase gradually after ignition. The pool fire is completely blocked by the

plate obstacle due to the smaller heat release rate. It should be noted that the flame appearance in that phase is consistent with the ceiling jet.

(2) The phase of stable burning. For that phase, the burning rate is approximately constant. The flame spreads horizontally over the lower surface of the plate obstacle before appearing above it. Compared with pool fire under the free burning condition, the flame width becomes larger for pool fire under the effect of plate obstacle.

(3) The phase of boiling burning. After a period of stable combustion, the burning rate would increase significantly. During that stage, it was seen that some bubbles were generated near the vessel wall continuously, the sound of the boiling appeared. More fuel vapor is produced and is burnt above the plate obstacle. It can be found that the flame envelops the plate obstacle nearly.

(4) The phase of decay. The phase appears at the end of burning. Similar to the first phase, the flame is nearly sheltered by the plate obstacle due to the smaller fuel vapor produced.

Fig. 5 illustrates the burning rates for n-heptane pool fires under the effect of plate obstacle. As shown in Table 2, some important burning parameters are calculated, where $\dot{m}_2''$ and $\dot{m}_3''$ are the burning rates for the phase of stable burning (II) and the phase of boiling burning (III), respectively. For the laboratory scale n-heptane pool fire in this research, the $\dot{m}_2''$ almost unchanges with the size or position of plate obstacle, meaning that the obstacle has limited effect on the stable burning stage.

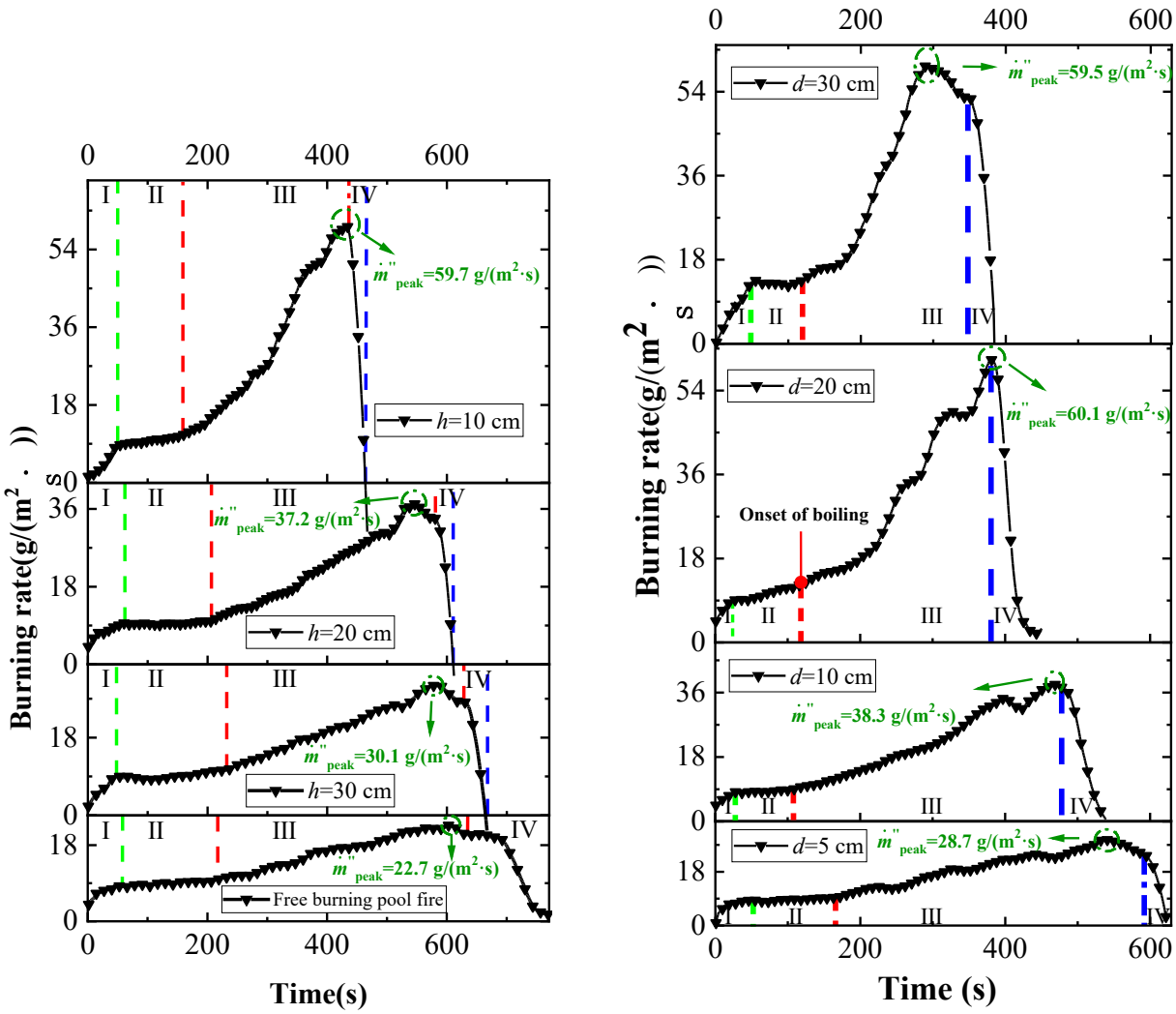

(a) Burning rate for plate obstacle (d=20 cm) (b) Burning rate for plate obstacle (h=5 cm)

Fig. 5 Burning rates for n-heptane pool fires under the effect of plate obstacle

Based on our research before [18], the fuel pool starts to boil when the temperature of burner bottom reaches the boiling point. It is found that the onset boiling time starts slightly earlier for n-heptane pool fire under the effect of plate obstacle with lower height, as shown in Table 2 and Fig. 5. As the h decreases or the d increases, the burning rate during the phase III ($\dot{m}''_3$) increases. For n-heptane pool fires sheltered by 60 cm and 10 cm height of the plate obstacle with same diameter, the burning rate increased from 18.4 g·m^{-2}·s^{-1} to 31.7

g·m^{-2}·s^{-1}. For 5 cm and 30 cm diameter plate obstacle (h= 20 cm), the burning rate of pool fire increases from 19.6 g·m^{-2}·s^{-1} to 37.2 g·m^{-2}·s^{-1}. Meanwhile, the peak burning rate increases significantly with decrease of the height of plate obstacle or increase of the plate obstacle diameter. When compared to pool fire under the free burning condition, the n-heptane pool fire with plate obstacle (d = 20 cm, h = 10 cm) has a larger peak heat release rate by factors of about 3. Moreover, when the h decreases or the d increases, the evolution of burning behavior would approach to that for pool fire under the free burning condition. The plate obstacle over the burner would result in a rapidly developing fire with higher burning rate.

Table 2 The parameter of burning behavior for n-heptane pool fire with plate obstacle

Plate obstacle diameter (cm)	**Plate obstacle height (cm)**	$\dot{m}''_2$ (g·m^{-2}·s^{-1})	$t_{boiling}$ (s)	$\dot{m}''_3$ (g·m^{-2}·s^{-1})	t_{peak} (s)	$\dot{m}''_{peak}$ (g·m^{-2}·s^{-1})	t_{total} (s)	$\dot{m}''_{average}$ (g·m^{-2}·s^{-1})
20	5	10.5	119	31.5	381	63.4	430	23.7
	10	9.7	157	31.7	432	59.7	449	22.8
	20	9.5	206	22.9	539	37.2	592	17.3
	30	9.1	232	20.8	565	30.1	692	14.8
	40	8.3	184	17.4	579	25.6	710	14.4
	60	9.1	243	18.4	537	25.4	716	14.3
5	5	8.6	161	19.6	533	28.7	629	16.2
10		8.4	217	22.4	402	38.3	553	18.5
20		10.5	121	31.5	381	60.1	430	23.7
30		13.0	119	37.2	294	59.5	376	27.1
Free burning		8.9	194	16.5	605	22.7	23.4	13.4

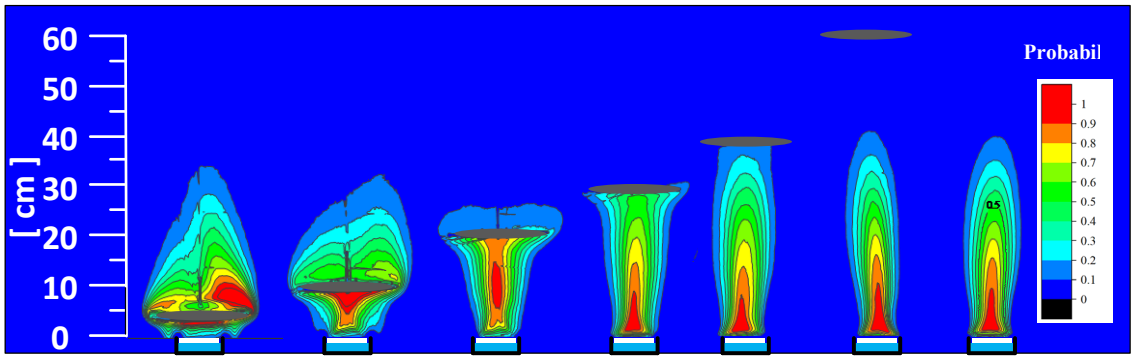

Fig. 6 The change of n-heptane pool fire morphological characteristics with different height of plate obstacle (d=20 cm)

Fig. 6 shows the change of n-heptane pool fire morphological characteristics with the height of plate obstacle, where the probability contour for pool fire was calculated over the entire burning time. It is found for the n-heptane pool fire, the decrease in the height dramatically changes the flame morphological characteristics, including flame geometry, flame width, flame height. When the obstacle height is low, i.e. h=5 cm, 10 cm, the plate splits the pool fire, and partial flame appears above the obstruction, implying that combustible vapor produced cannot be completely burnt beneath the obstruction. The flame width is larger because of the flame spread along the plate, while the flame height is slightly lower due to the inhibitory effect of obstacles. When the obstacle height is h=20 cm, 30 cm, most flame is blocked below by obstacles, forming a ceiling jet. As the h decreases or the d increases, the flame geometry approach to that for pool fire under the free burning condition. The quantitative influence of obstacle on the pool fire appearance needed to be further studied.

3.2 Mean burning rate

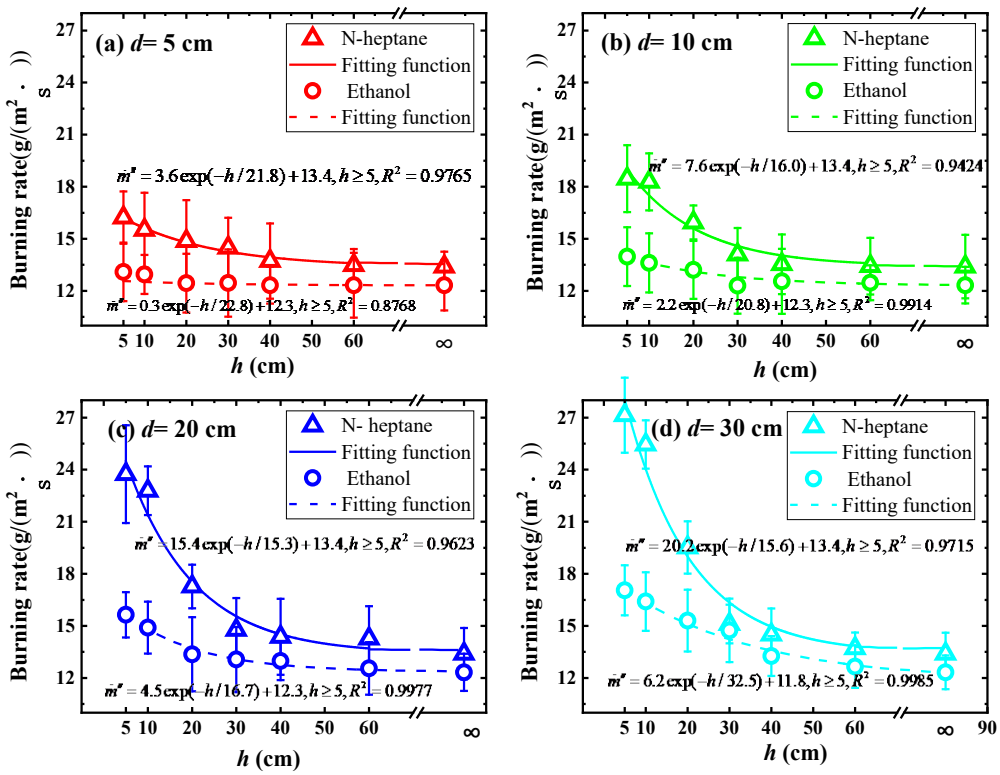

Fig. 7 The mean burning rates of pool fires vs. the height of plate obstacle

The variation of mean burning rates with the height of plate obstacle is shown in Fig. 7. An increasing trend of the mean burning rate is demonstrated with the increasing *d* and the decreasing *h*. The increase of burning rate induced by plate obstacle is larger for n-heptane pool fire when compared to ethanol pool fire. Furthermore, as the *h* increases or the *d* decreases, the value of mean burning rate would approach to the value for pool fire under the free burning condition, and the values for n-heptane and ethanol are 13.4 $g\cdot m^{-2}\cdot s^{-1}$ and 12.33 $g\cdot m^{-2}\cdot s^{-1}$, respectively. Similarly, it could be inferred that, the burning rate would close to the value of pool fire under the free burning condition when the geometrical dimension of the plate obstacle is small enough.

In order to obtain the quantitative formula between the mean burning rate and the parameter of plate obstacle, the data is fitted using exponential decay function as shown in Fig. 7, where the R^2 is the coefficient of determination in the field of statistics. The coefficient in the fitted exponential decay function changes with fuel type or the geometrical dimension of the plate obstacle, so it is necessary to introduce a global model to explain the influence of plate obstacle, which would be described further.

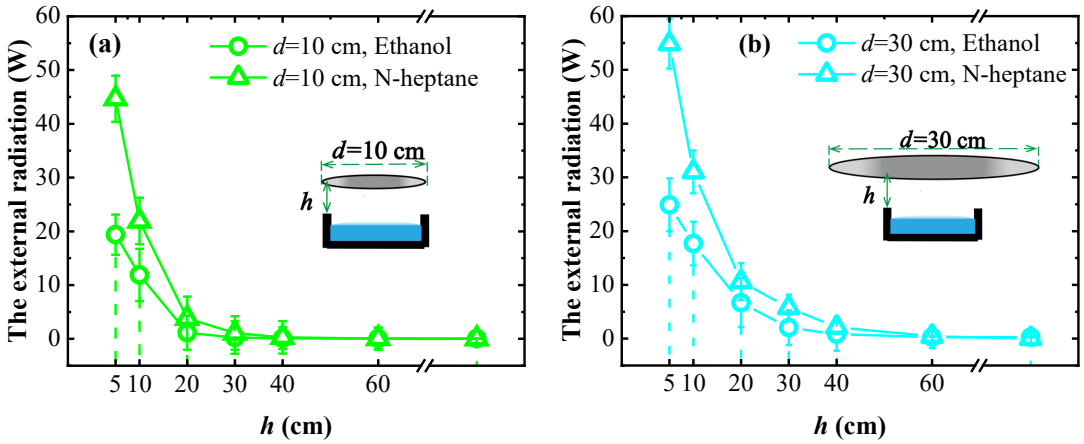

Fig. 8 The external radiation from the plate obstacle

In order to explain the change of burning rate, the heat transfer for pool fire sheltered by plate obstacle was calculated to based on the proposed theoretical analysis in Section 2. In the calculation, the emissivity of plate obstacle was assumed to be 1, and the average temperature of plate obstacle from three measurement points (T1, T2, T3) was considered as the characteristic temperature. The external radiation from the plate obstacle was obtained for both n-heptane and ethanol pool fires.

As shown in the Fig. 8, the external radiation from the plate obstacle to fuel surface increases with increasing geometrical dimension of the plate obstacle, and increases with decreasing height of plate obstacle. It is expected that the external radiation of n-heptane

pool fire is larger than that of ethanol pool fire, owing to that the heptane fire has a greater heat release rate. As expressed in the Eq. (5), the external radiation depends on the temperature and view factor. When the height of plate obstacle decrease, the decreasing distance between flame and plate obstacle would enhance the heat transfer from flame to the obstacle, which leading to the high temperature of plate obstacle. For n-heptane pool fire with higher heat release rate, the larger flame volume increases the heat exchange area with plate obstacle, resulting in higher temperature of the plate surface. It is found that the value of external radiation approach 0 when the h exceeds the flame height of pool fire under the free burning condition, where the flame heights for 10 cm diameter heptane and ethanol pool fire are about 40 cm and 26 cm, respectively. Otherwise, the view factor in the Eq. (6) would increase with increasing d, and decreasing h.

Fig. 9 shows the comparison of the increased burning rate between the experimental measurement and predicted value. The error between the experimental result and the predicted value is approximately 20%. It could be speculated that the burning rate enhancement influenced by the plate obstacle is mainly due to the external radiation from plate obstacle. The experimental value is slight larger than the theoretical value, owing to that the influence of plate obstacle on conduction item and convection item is ignored in the assumption. As shown flame appearance in the Fig. 2, it is found that more combustion occurs in the space between burner and plate obstacle, and leads to the increase of flame temperature near the fuel pan i.e. T_f. Otherwise, due to the blocking effect of obstacles, the flow field around the fuel pool becomes complex and turbulent, and results in the increase convective heat transfer coefficient, i.e. h_f. Based on the Eqs. 2-3, it can be inferred that

$\dot{q}''_{\text{cond}}$ and $\dot{q}''_{\text{conv}}$ would increase under the effect of the plate obstacle, which leads to the differences between experimental data and theoretical data.

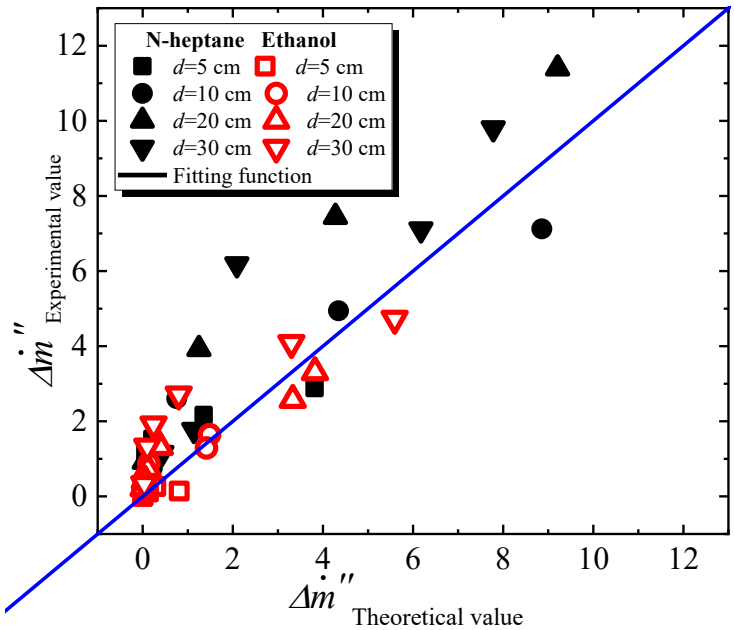

Fig. 9 Comparison of the increased burning rate between the experimental measurement and predicted value

To characterize burning rate of pool fire affected by plate obstacle, a dimensionless study was performed. The nondimensional parameters for the size and position of plate obstacle could be written as d/D and h/D, where D is the burner diameter. Moreover, it is also found that the fuel type has significant influence on pool fire with plate obstacle. The diffusive transfer B number written as H_c/H_g is the ratio of the heat of combustion to the latent heat of gasification, which is introduced as a nondimensional parameter to represent the effect of fuel type. The non-dimensional ratio of the increased burning rate to burning rate of pool fire under the free burning condition can be expressed by following function

$$\Delta\dot{m}''/\dot{m}_0'' = f(d/D, h/D, B) \tag{8}$$

The B number is found to be proportional to the burning rate for pool fire with different fuel. According to the thermal properties listed in the Table 1, the B number is calculated as 98 for the heptane pool fires and 30 for the ethanol pool fires, respectively. For the same obstacle condition, the pool fire with larger B number would release more heat, resulting in higher temperature of the plate surface, which leads to the more obvious influence on burning characteristics. Besides, the burner diameter is constant in the current study. So the Eq. (8) could be converted to

$$\Delta\dot{m}''/\dot{m}_0'' = f(h/d \times B) \tag{9}$$

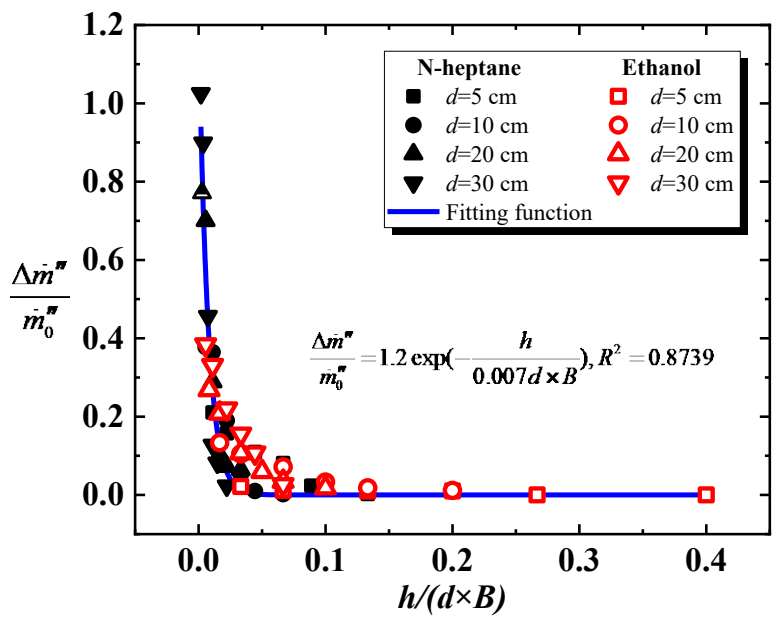

Fig. 10 The dimensionless increased burning rate vs. the value of *h/(d ×B)*

All experimental data for heptane and ethanol pool fires under the effect of plate obstacle is fitted using the exponential decay function in the Fig. 10. The relationship between dimensionless increased burning rate and *h/(d ×B)* can be obtained

$$\Delta \dot{m}''/\dot{m}_0'' = 1.2\exp(-h/0.007d \times B), R^2 = 0.87 \quad (10)$$

It can be seen that dimensionless increased burning rate decreased with dimensionless parameter, i.e. *h/(d ×B)*. Specially under an extreme condition, if the *h* is infinitely larger or the diameter of plate obstacle is infinitely small, this approaches the infinity. That will result in that the burning rate for pool fire under the effect of plate obstacle would close to that of a pool fire under the free burning condition, or dimensionless increased burning rate approach 0. In addition, this relationship also incorporates the influence of fuel properties. It should be noted that the influence of burner diameter and the obstacle material on burning rate requires further verification.

3.3 Mean radiation heat flux

In fire scenarios, radiation emitted from flame may ignite surrounding combustibles and even cause a domino effect, so the radiation heat flux is an important parameter in fire safety. Fig. 11 presents the measured radiation heat flux evolution with time for n-heptane pool fire under the effect of plate obstacle and pool fire under free burning condition, where radiometer positioned at 60 cm from the fire axis. It is expected that the radiation heat flux evolution follows the burning rate, and the plate obstacle above the burner has a considerable effect on the radiation heat flux. The plate obstacle would lead to rapidly developing fire with higher radiation heat flux.

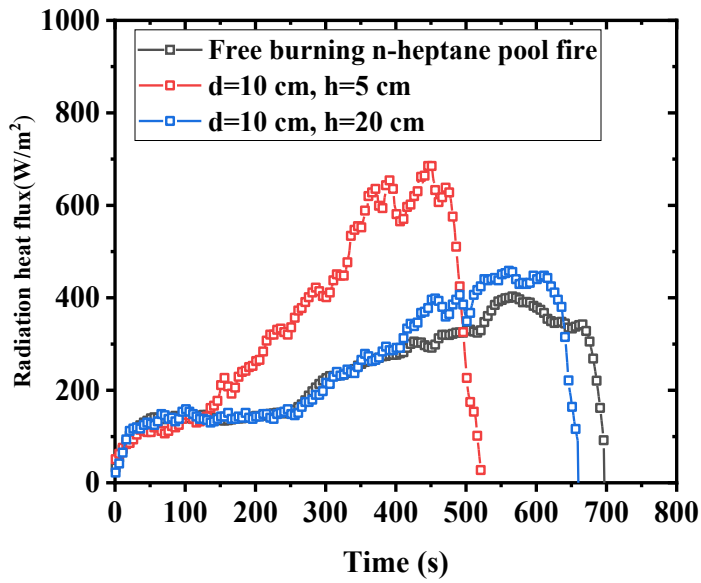

Fig. 11 Radiation heat flux evolution with time for n-heptane pool fire under the effect of plate obstacle

The mean radiation heat flux i.e. $\dot{q}''_{mean}$ is proportional to the burning rate, which is found to be related with the characteristics of plate obstacle, i.e. *h/d*. As shown in Fig. 12, $\dot{q}''_{mean}$ could be correlated with *h/d* for n-heptane and ethanol pool fires. The obtained formula can be written as

$$\dot{q}''_{mean} = 212.9 + 189.6\exp(-h/1.1d) \quad \text{for n-heptane pool fire}$$

$$\dot{q}''_{mean} = 104.6 + 37.0\exp(-h/2.0d) \quad \text{for ethanol pool fire} \tag{11}$$

The influence of plate obstacle on the $\dot{q}''_{mean}$ is remarkable for the n-heptane pool fire, which could be caused by the various characteristic in their flame sooty and emissivity. It should be noted that radiation of pool fire would change with scale due to smoke blocking effect, the obtained relationship requires further verification.

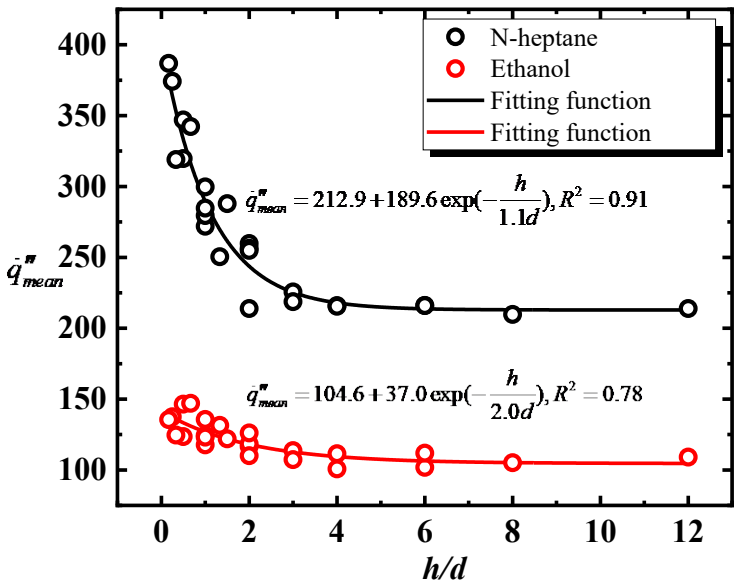

Fig. 12 The mean radiation heat flux vs. the value of *h/d*

4. Conclusions

Aiming at characterizing the influence of a plate obstacle on pool fire, a series of small-scale pool fires sheltered by plate obstacle are carried out experimentally, where the pool fire under the free burning condition are conducted as the contrast. The main conclusions are:

(1) The plate obstacle above the burner has a considerable effect on the burning behaviors of n-heptane and ethanol pool fires. The plate obstacle over the burner would result in a rapidly developing fire with higher burning rate. When compared to pool fire under the free burning condition, the n-heptane pool fire with plate obstacle (d = 20 cm, h = 10 cm) has a larger peak heat release rate by factors of about 3.

(2) An increasing trend of the mean burning rate is demonstrated with the improving diameter of the plate obstacle and the decreasing height of the plate obstacle, which is more obvious for heptane pool fire due to more heat transfer between flame and plate obstacle.

Based on the heat transfer analysis for pool fire with plate obstacle, the burning rate enhancement is found to mainly result from the external radiation from plate obstacle.

(3) Based on theoretical and scaling analysis, the burning rate is determined by the obstacle scale i.e. d/D, the obstacle position i.e. h/D, the fuel property i.e. H_c/H_g. A new correlation is further obtained from the experimental data of heptane and ethanol pool fires to describe the effect of plate obstacle, expressed as $\Delta\dot{m}''/\dot{m}_0'' = 1.2\exp(-h/0.007d \times B)$.

(4) The plate obstacle could contribute to a higher radiation heat flux, where the influence on radiation heat flux is remarkable for the n-heptane pool fire due to the more flame sooty. Besides, the relationship between mean radiation heat flux and the characteristics of plate obstacle follows the exponential decay function.

Acknowledgements

The authors (except Wai Cheong Tam) would like to acknowledge financial support sponsored by National Natural Science Foundation of China (No. 51874344; No. 51874255; No. 52174209), Fundamental Research Funds for the Central Universities (No. 20CX06068A, No. 19CX07006A), and Qingdao Postdoctoral Science Foundation Funded Project (No. qdyy20200095).

Reference:

[1] Pan L, Liu P, Li Z. A system dynamic analysis of China's oil supply chain: Over-capacity and energy security issues. Appl. Energy. 2017;188:508-20.

[2] Deng L, Tang F, Wang X. Uncontrollable combustion characteristics of energy storage oil pool: Modelling of mass loss rate and flame merging time of annular pools. Energy. 2021;224:120181.

[3] Abdalla AM, Hossain S, Nisfindy OB, Azad AT, Dawood M, Azad AK. Hydrogen production, storage, transportation and key challenges with applications: A review. Energy Conv. Manag. 2018;165:602-27.

[4] Sepehri A, Sarrafzadeh M-H. Effect of nitrifiers community on fouling mitigation and nitrification efficiency in a membrane bioreactor. Chem. Eng. Process. 2018;128:10-8.

[5] Li M, Shu Z, Yi L, Chen B, Zhao Y, Geng S. Combustion behavior and oscillatory regime of flame spread over ethanol aqueous solution with different proportions. Fuel. 2019;253:220-8.

[6] Ding Y, Huang B, Li K, Du W, Lu K, Zhang Y. Thermal interaction analysis of isolated hemicellulose and cellulose by kinetic parameters during biomass pyrolysis. Energy. 2020;195:117010.

[7] Li M, Zhang C, Wang C, Liu Z, Wang B. Ignition behavior and critical distance of flammable liquids by radiant heat flux from adjacent pool fire. Int. J. Therm. Sci. 2021;168:107043.

[8] Falkenstein-Smith R, Sung K, Chen J, Hamins A. Mixture fraction analysis of combustion products in medium-scale pool fires. Proc. Combust. Inst. 2021;38(3):4935-42.

[9] Yang R, Khan F, Neto ET, Rusli R, Ji J. Could pool fire alone cause a domino effect? Reliab. Eng. Syst. Saf. 2020;202:106976.

[10] Yu L, Wan H, Gao Z, Ji J. Study on flame merging behavior and air entrainment restriction of multiple fires. Energy. 2021;218:119470.

[11] Shi C, Liu W, Hong W, Zhong M, Zhang X. A modified thermal radiation model with multiple factors for investigating temperature rise around pool fire. J. Hazard. Mater. 2019;379:120801.

[12] Shen G, Zhou K, Wu F, Jiang J, Dou Z. A model considering the flame volume for prediction of thermal radiation from pool fire. Fire Technology. 2019;55(1):129-48.

[13] Ding L, Gong C, Ge F, Ji J. Experimental study on flame radiation characteristic from line pool fires of n-heptane fuel in open space. Energy. 2021;218:119435.

[14] Ji J, Gong C, Wan H, Gao Z, Ding L. Prediction of thermal radiation received by vertical targets based on two-dimensional flame shape from rectangular n-heptane pool fires with different aspect ratios. Energy. 2019;185:644-52.

[15] Li M, Shu Z, Chen B, Wang C, Geng S, Han G. Influence of pool width on pioneering flame height of flame spread over jet fuel inside a bench-scale air flow tunnel. Tunnelling and Underground Space Technology. 2021;108:103763.

[16] Li M, Han G, Yang S. Experimental investigation on flame morphology and improved flame radiation model of rectangular heptane pool fire. Process Saf. Environ. Protect. 2021.

[17] Blinov VI, Khudyakov GN. Diffusion Burning of Liquid, Army Engineer Research and Development Labs Fort Belvoir VA. 1961.

[18] Chen B, Lu S, Li C, Kang Q, Lecoustre V. Initial fuel temperature effects on burning rate of pool fire. J. Hazard. Mater. 2011;188(1):369-74.

[19] Kong D, Zhang Z, Ping P, He X, Yang H. Effects of the initial fuel temperature on burning behavior of crude oil pool fire in ice cavities. Experimental Heat Transfer. 2018;31(5):436-49.

[20] Zhang Z, Zong R, Tao C, Ren J, Lu S. Experimental study on flame height of two oil tank fires under different lip heights and distances. Process Saf. Environ. Protect. 2020;139:182-90.

[21] Deng L, Tang F, Ma X. Experimental study on flame merging probability and pulsation frequency of annular hydrocarbon pool fires with various inner and outer diameters. Process Saf. Environ. Protect. 2021;146:473-80.

[22] Tao C, Liu Y, Tang F, Wang Q. An experimental investigation of the flame height and air entrainment of ring pool fire. Fuel. 2018;216:734-7.

[23] Kong D, Zhang Z, Ping P, Chen G, He X, Yang H. Experimental study on burning behavior of crude oil pool fire in annular ice cavities. Fuel. 2018;234:464-72.

[24] Liu J, Zhou Z. Examination of radiative fraction of small-scale pool fires at reduced pressure environments. Fire Saf. J. 2019;110:102894.

[25] Fang J, Wang J, Tu R, Shang R, Zhang Y, Wang J. Optical thickness of emissivity for pool fire radiation. Int. J. Therm. Sci. 2018;124:338-43.

[26] Fang J, Tu R, Guan J-f, Wang J-j, Zhang Y-m. Influence of low air pressure on combustion characteristics and flame pulsation frequency of pool fires. Fuel. 2011;90(8):2760-6.

[27] Chen J, Zhao Y, Bi Y, Li C, Kong D, Lu S. Effect of initial pressure on the burning behavior of ethanol pool fire in the closed pressure vessel. Process Saf. Environ. Protect. 2021;153:159-66.

[28] Chen Y, Hu L, Kuang C, Zhang X, Lin Y, Zhong X. Flame interaction and tilting behavior of two tandem adjacent hydrocarbon turbulent diffusion flames in crosswind: An experimental quantification and characterization. Fuel. 2021;290:119930.

[29] Hu L, Hu J, Liu S, Tang W, Zhang X. Evolution of heat feedback in medium pool fires with cross air flow and scaling of mass burning flux by a stagnant layer theory solution. Proc. Combust. Inst. 2015;35(3):2511-8.

[30] Kuang C, Hu L, Zhang X, Lin Y, Kostiuk LW. An experimental study on the burning rates of n-heptane pool fires with various lip heights in cross flow. Combust. Flame. 2019;201:93-103.

[31] Chen J, Zhang X, Zhao Y, Bi Y, Li C, Lu S. Oxygen concentration effects on the burning behavior of small scale pool fires. Fuel. 2019;247:378-85.

[32] Li Z, Zhang P. Fire behaviors of fuels with different sootiness levels in hot and humid conditions. Process Saf. Environ. Protect. 2021;146:350-9.

[33] Wang C, Ding L, Wan H, Ji J, Huang Y. Experimental study of flame morphology and size model of a horizontal jet flame impinging a wall. Process Saf. Environ. Protect. 2021;147:1009-17.

[34] Wang Z, Zhou K, Zhang L, Nie X, Wu Y, Jiang J, et al. Flame extension area and temperature profile of horizontal jet fire impinging on a vertical plate. Process Saf. Environ. Protect. 2021;147:547-58.

[35] Chen J, Zhao Y, Chen X, Li C, Lu S. Effect of pressure on the heat transfer and flame characteristics of small-scale ethanol pool fires. Fire Safety Journal. 2018;99:27-37.

[36] Thermophysical Properties: Ethanol, (2018) https://www.thermalfluidscentral.org/encyclopedia/index.php/Thermophysical_Properties: Ethanol , Accessed date: 16 July 2018. .

[37] Thermophysical Properties: Heptane, (2018) https://www.thermalfluidscentral.org/encyclopedia/index.php/Thermophysical Properties: Ethanol , Accessed date: 16 July 2018.

[38] Bergman TL, Bergman TL, Incropera FP, Dewitt DP, Lavine AS. Fundamentals of heat and mass transfer: John Wiley & Sons, 2011.

[39] Sung K, Chen J, Bundy M, Hamins A. The characteristics of a 1 m methanol pool fire. Fire Saf. J. 2021;120:103121.

[40] Moffat RJ. Describing the uncertainties in experimental results. Exp. Therm. Fluid Sci. 1988;1(1):3-17.

[41] Chen J, Tam WC, Tang W, Zhang C, Li C, Lu S. Experimental study of the effect of ambient pressure on oscillating behavior of pool fires. Energy. 2020;203:117783.

[42] Li B, Wan H, Gao Z, Ji J. Experimental study on the characteristics of flame merging and tilt angle from twin propane burners under cross wind. Energy. 2019;174:1200-9.